DOI: 10.1002/chem.200902712

Spontaneous Hierarchical Assembly of Crown Ether-like Macrocycles into Nanofibers and Microfibers Induced by Alkali-Metal and Ammonium Salts

Joseph K.-H. Hui,[a] Peter D. Frischmann,[a] Chien-Hsin Tso,[b] Carl A. Michal,[b] and Mark J. MacLachlan*[a]

Abstract: Schiff base macrocycle **1**, which has a crown ether like central pore, was combined with different alkali-metal and ammonium salts in chloroform, resulting in one-dimensional supramolecular aggregates. The ion-induced self-assembly was studied with solid-state NMR spectroscopy, transmission electron microscopy (TEM), scanning electron microscopy (SEM), and atomic force microscopy (AFM). It was found that the lengths and widths of the superstructures depend on the cation and counteranion of the salts. Among the salts being used, Na^+ and NH_4^+ ions with BF_4^- ions showed the most impressive fibrous structures that can grow up to 1 μm in diameter and hundreds of microns in length. In addition, the size of the fibers can be controlled by the evaporation rate of the solvent. A new macrocycle with bulky triptycenyl substituents that prevent supramolecular assembly was prepared and did not display any nanofibers with alkali-metal ions in chloroform when studied with TEM.

Keywords: coordination polymers · electrostatic interactions · hierarchical assembly · macrocycles · Schiff bases

Introduction

For many years, chemists have been looking to nature for inspiration in the development of new materials.[1] Natural materials such as cellulose[2] and spider silk[3] acquire their remarkable properties from the exquisite hierarchical organization of biomolecules, often extending over several length scales. For instance, collagen is a fibrous protein found in connective tissue[2,4] (e.g., ligaments, skin, cartilage) and is the most abundant protein in mammals. Its usefulness arises from a complex, hierarchical structure whereby peptide chains organize into tropocollagen helices, which assemble into microfibrils, then aggregate into macrofibrils and even bundles of macrofibrils.[5] While synthesis of small molecules and crystalline solids is well-developed, understanding and controlling the self-assembly of molecules into organized materials is still in its infancy.

The highly sophisticated organization of biomaterials is daunting to molecular chemists, but it is clear that understanding and harnessing the assembly of matter over several length scales will present opportunities for crafting innovative materials with advanced functions. Taking advantage of weak intermolecular interactions, such as π–π stacking, hydrogen bonding, and coordination bonding, as well as hydrophobic effects, chemists have developed many beautiful structures,[6,7] but rarely do these exhibit multiscale hierarchical assembly.

The organization of shape-persistent macrocycles into supramolecular structures is a promising way to develop new functional materials,[8] such as liquid crystals[9] and ion channels.[10] There are several reports of self-assembled fibers from shape-persistent macrocycles by using hydrogen bonding and π stacking,[11] but alkali metals, where ionic interactions dominate, have not often been used to mediate the formation of supramolecular polymers.[12] This exclusion likely arises from the difficulties of controlling ionic interactions—they are nondirectional and can act over a long distance. Höger et al. reported discrete dimers constructed from charged shape-persistent macrocycles, but these did not further organize.[13] Davis et al. reported charged assemblies of calix[4]arene appended with four guanosine sub-

[a] J. K.-H. Hui, P. D. Frischmann, Prof. Dr. M. J. MacLachlan
Department of Chemistry, University of British Columbia
2036 Main Mall, Vancouver, BC, V6T 1Z1 (Canada)
Fax: (+1) 604-822-2847
E-mail: mmaclach@chem.ubc.ca

[b] C.-H. Tso, Prof. Dr. C. A. Michal
Department of Physics and Astronomy
University of British Columbia
6224 Agricultural Rd., Vancouver, BC, V6T 1Z1 (Canada)

Supporting information for this article is available on the WWW under http://dx.doi.org/10.1002/chem.200902712.

stituents upon the addition of $NaBPh_4$ in which the Na^+ is located at the inner core of the cation-filled channel.[14] However, it was the intermolecular hydrogen bonding of the neighboring guanosine units that led to aggregation. Electrostatic interactions have often been used to assemble multilayer thin films[15] and block copolymers,[16] but rarely in the formation of nanofibers with macrocyclic materials.[17] Controlling the level of hierarchical self-assembly of nanofibers remains a big challenge.[18]

Biomolecules are often used as models for supramolecular assembly, and their organization can be facilitated by alkali cations. For instance, guanosine, a nucleoside comprising guanine attached to a ribose ring, can self-assemble into macrocyclic hydrogen-bonded tetramers (G-quartets) that are templated by alkali metal ions, namely Na^+ and K^+; the tetramers further stack vertically into columns with the cations being sandwiched between the layers of G-quartets.[19] This alkali-metal ion-induced assembly yields hydrogels that are promising candidates for applications such as stimuli-responsive materials and sensors.[19,20] A related G-quartet based on 5′-guanosine monophosphate (5′-GMP) has been shown to assemble into stacks, leading to G-quadruplexes.[21] Guanine-rich DNA segments have also been shown to assemble into extended structures with embedded ion channels through alkali- and alkaline-earth metal ion assembly.[22] These studies of biological self-assembly are important for developing new biosensors, and for understanding ion transport in natural systems.

Here we report on the supramolecular assembly of Schiff base macrocycles into polymers, nanofibers, and further into microfibrils. This multi-level hierarchical assembly is supported by micrographs and spectroscopic evidence for the structure, which is similar to the structural organization observed in guanosine-based fibers.

Results and Discussion

Schiff base macrocycle **1**[23] is a conjugated molecule that resembles [18]crown-6 in the arrangement of six oxygen atoms in its interior. In contrast to crown ethers, however, the rigid backbone of macrocycle **1** prevents it from distorting sufficiently to offer an octahedral binding site for Na^+. Previously, we have shown that addition of $NaBPh_4$ and other alkali-metal tetraphenylborate salts to macrocycle **1** gives a spectroscopic signature for aggregation in solution.[24] With the addition of Na^+, the color of the solution changes from orange to red, and the ^1H NMR spectrum of macrocycle **1** shows large upfield changes in the resonances assigned to the aromatic protons. These shifts are consistent with the formation of a 1D assembly in solution, where the macrocycles are stacked on top of one another to share binding of the hydroxyl groups to the Na^+. Moreover, we observed aggregates in solution by electrospray ionization mass spectrometry (ESI-MS). The use of tetraphenylborate anion was necessary to maintain solubility of the assemblies for solution-based studies.

When a solution of macrocycle **1** in chloroform was treated with excess of $NaBF_4$ (itself nearly insoluble in chloroform), a color change from orange to deep red was observed. The excess salts were filtered, and the solution became noticeably viscous after a few minutes (no gel formed, but a precipitate formed after standing for several minutes). Dynamic light scattering (DLS) revealed a particle size of approximately 50 nm and the ^1H NMR signals were broadened and shifted upfield, indicating aggregation of the macrocycles. Samples were dried on transmission electron microscopy (TEM) grids. Figure 1a and b show TEM images of $[Na\cdot\mathbf{1}]BF_4$ (composition confirmed by elemental analysis). Surprisingly, the sample is organized into a fibrous morphology, where the diameters of the fibers are around 170 nm, considerably larger than the diameter of macrocycle **1** (ca. 2–3 nm). Scanning electron microscopy (SEM) also re-

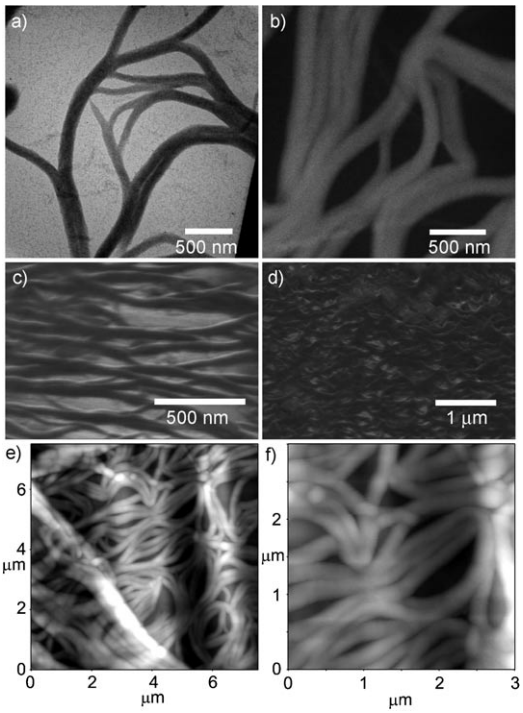

Figure 1. a, b) TEM, c, d) SEM, and e, f) AFM images of $[Na\cdot\mathbf{1}]BF_4$. All samples were prepared by drop-casting a chloroform solution of $[Na\cdot\mathbf{1}]BF_4$ onto formvar carbon-coated grids (TEM and AFM) or aluminum stubs (SEM) and dried at ambient condition.

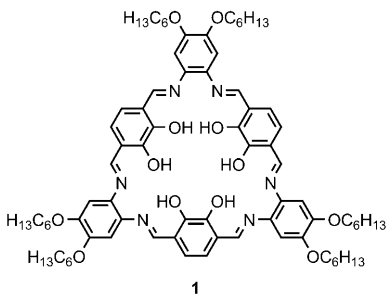

1

vealed the 3D structure of the fibers in the sample (see Figure 1c and d). The bundles appear cylindrical in shape. Atomic force microscopy (AFM) in tapping mode showed that the samples are relatively smooth and approximately of the same size as observed by TEM (see Figure 1e and f). Attempts to obtain images in contact mode resulted in sample destruction typical of soft materials. Similar structures were observed with a shorter chain analogue of macrocycle **1** (e.g., with butyloxy substituents) when combined with $NaBF_4$.

As the formation of this fiber morphology was unexpected, we explored the parameters in the assembly. First, to verify that the assembly required the salt, control experiments were conducted by dissolving the macrocycle in chloroform, filtering, and evaporating on a TEM grid. Electron microscopy showed no fiber structures over several attempts (see Figure S1 in the Supporting Information). With $NaBF_4$ in the experiment, nanofibers were always observed.

Second, to prove that this was not simply phase separation of the components during evaporation, a powder X-ray diffraction (PXRD) pattern of a sample of [Na·**1**]BF_4 was compared with those of $NaBF_4$ and macrocycle **1** (prepared in the same way). Figure 2a shows the PXRD patterns of these three samples. $NaBF_4$ is a microcrystalline powder with no peaks at low angle and macrocycle **1** is microcrystalline with peaks between $2\theta = 5°$ and 30°. The PXRD pattern of [Na·**1**]BF_4 shows a completely different pattern clearly contradicting simple phase separation of the components. The peaks for [Na·**1**]BF_4 are reproducible and index to a high symmetry (likely orthorhombic) lattice with large unit cell parameters, but a definitive unit cell could not be found as there are too few peaks observed. The peaks are at low angle (ca. 35 Å d spacing) where peaks arising from interstack separations in a columnar organization of macrocycles would be expected.

To obtain further information about the role of the salt in the supramolecular assembly, we undertook solid-state NMR investigations. ^{23}Na NMR spectra of [Na·**1**]BF_4 revealed that ^{23}Na experiences a large quadrupole coupling in the complex. As shown in Figure 3a, proton decoupling sharpens the ^{23}Na resonance considerably. Proton decoupling applied to a sample of [Na·**1**]BF_4 where the hydroxyl protons were exchanged with deuterons produces a much less pronounced change (Figure 3b). These data provide strong evidence that the Na^+ cations reside on the interior of the macrocycle, bonded to the hydroxyl groups. The hydroxyl deuteron is evidently highly labile, as it readily exchanged with ^1H from atmospheric humidity. ^{19}F decoupling produced no change in the spectra, indicating a substantial (>4 Å) separation between the Na^+ cations and the BF_4^- anions. The room temperature ^2H NMR spectrum shows a featureless broad line without any obvious singularities as would be expected from a well defined ^2H quadrupole coupling (Figure 3c). Cooling the sample to −50 °C produces changes to the line shape that suggest some motional averaging is taking place. ^{11}B NMR spectroscopy revealed a

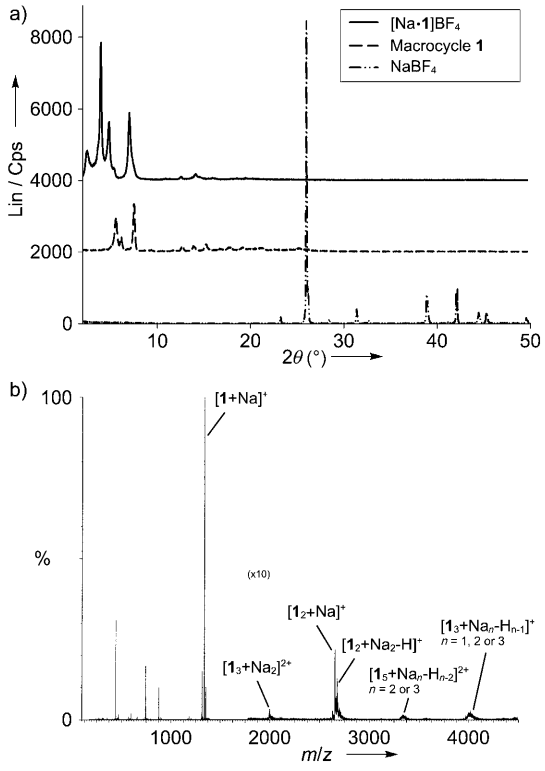

Figure 2. a) PXRD pattern of the macrocycle **1**, $NaBF_4$ and [Na·**1**]BF_4. b) ESI-MS of [Na·**1**]BF_4.

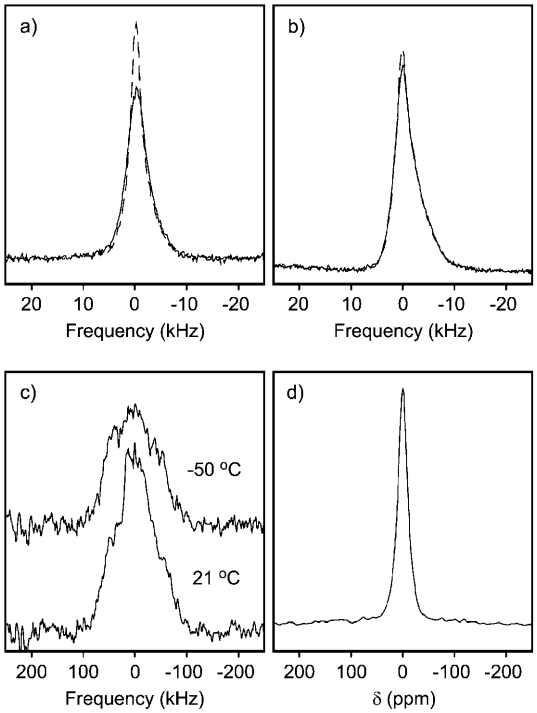

Figure 3. Solid-state ^{23}Na NMR spectra acquired with and without proton decoupling (dashed line and solid line, respectively) of a) [Na·**1**]BF_4 and b) [Na·**1**]BF_4 with hydroxyl deuterons. c) Solid-state ^2H NMR spectra acquired at $T = 21$ and −50 °C. d) Solid-state ^{11}B NMR spectrum of [Na·**1**]BF_4.

single, relatively sharp (2.4 kHz full-width at half-maximum) peak for the BF_4^- anions in [Na•**1**]BF_4 (Figure 3d). A similar spectrum acquired from powdered $NaBF_4$ (not shown) reveals a sharp (4 kHz) peak due to the central transition on top of a broad (100 kHz) powder pattern arising from the ^{11}B quadrupole coupling. The absence of the ^{11}B quadrupole coupling in [Na•**1**]BF_4, along with the dramatically different T_1 relaxation time (0.4 s, compared to 22.4 s in $NaBF_4$) indicates that the BF_4^- anions are rapidly tumbling in the nanofibers. A simple calculation incorporating ^{11}B quadrupolar relaxation and ^{11}B–^{19}F dipolar relaxation in the short-correlation time limit suggests a rotational correlation time in the order of 86 ns for the BF_4^- in the nanofibers.

Based on these data, we postulate that Na^+ first coordinates to the hydroxyl groups inside the macrocycles to initiate the formation of a polymer in solution (in a 1:1 ratio). This is also supported by the light scattering data, the ^1H NMR shifts, and observation of oligomers by electrospray ionization mass spectrometry (ESI-MS) of macrocycle **1** upon addition of $NaBF_4$ (see Figure 2b).

We attempted to exchange both the anion and cation of the nanofibers, and then examined them by energy dispersive X-ray (EDX) analysis. TEM grids with fibers of [Na•**1**]BF_4 were immersed in saturated aqueous solutions of $NaPF_6$ or KPF_6, followed by repeated rinsing with water. An EDX measurement was first performed on the fibers with [Na•**1**]BF_4 as a control and the signals corresponding to carbon, oxygen, fluorine, and sodium can be seen in the spectrum (the signal of boron could not be observed because it was hidden underneath the signal of carbon). The EDX spectra obtained from the samples exchanged with the PF_6^- salts showed the same pattern as the control plus a new signal attributed to phosphorus of the counter anion, suggesting that some of the surface anions of the fibers could be exchanged. However, when KPF_6 was used for the wash, no K^+ was observed by EDX, indicating that the Na^+ in the fibers is not readily exchanged. These results support the presence of tightly bound cations inside the fibers with exchangeable anions around the periphery.

If the macrocycles are stacked on top of one another with Na^+ bridging, then introducing bulky substituents should block the assembly. To test this, we first prepared the new compound 1,4-diformyl-2,3-dihydroxytriptycene (**4**) as shown in Scheme 1. Reaction of **4** with 4,5-dihexyloxyphenylenediamine (**3**) afforded macrocycle **2** in 51% yield (Scheme 1). The structure of the new macrocycle with bulky triptycenyl substituents was verified by NMR spectroscopy, mass spectrometry, and elemental analysis. Under identical experimental conditions employed for the assembly of macrocycle **1**, macrocycle **2** displayed no evidence of columnar aggregation (^1H NMR) for binding to either $NaBPh_4$ or $NaBF_4$, supporting the assertion that the stacking is important in the assembly of the polyelectrolyte. In the case of macrocycle **2**, the bulky triptycenyl groups prevent columnar assembly and, therefore, no fibrous structure was observed.

The polymer from macrocycle **1** and Na^+ is a highly charged rod-like assembly with the anions located outside of the macrocycles, but electrostatically bound to the positively charged polymer. We do not know the exact length of the polymers, but light scattering measurements suggest they are quite long at this stage in solution (an average size of 50 nm was observed, assuming a spherical shape). During evaporation and concentration,[25] the charge-balancing anions are attracted to other positively charged rods and the assembly organizes into nanofibers. Overall, the Na^+ ions are bound inside the macrocycle assembly, but the BF_4^- ions are only loosely bound, consistent with the solid-state NMR data and EDX analysis.

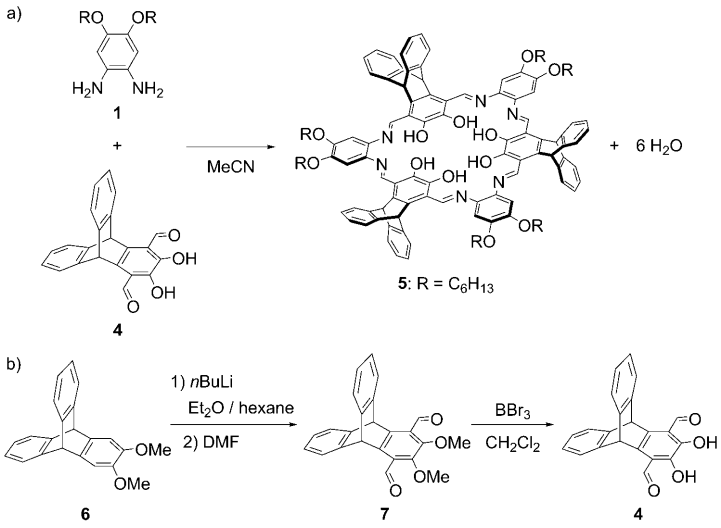

Scheme 1. a) Synthesis of macrocycle **2**. b) Synthesis of 1,4-diformyl-2,3-dihydroxytriptycene (**4**).

When larger anions were employed (e.g., BPh_4^-), the fibers obtained were of much lower quality—they were short and poorly defined (Figure 4). This is also consistent with our model where the anions are situated between the charged polymer rods, and large anions would be expected to disrupt the organization.

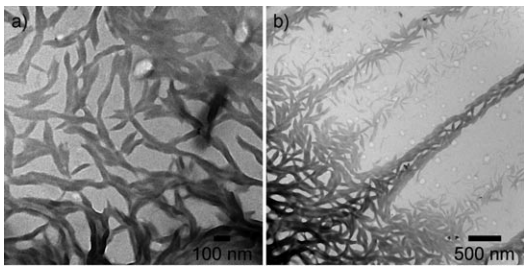

Figure 4. TEM images of macrocycle **1** with $NaBPh_4$.

In an effort to control the fiber growth, evaporation was conducted at different rates. TEM images of samples prepared with rapid evaporation revealed short fibers (see Figure 5). In contrast, very long, well-organized fibers were obtained with slow evaporation rates. These fractal structures, obtained from molecular assembly, resemble morphol-

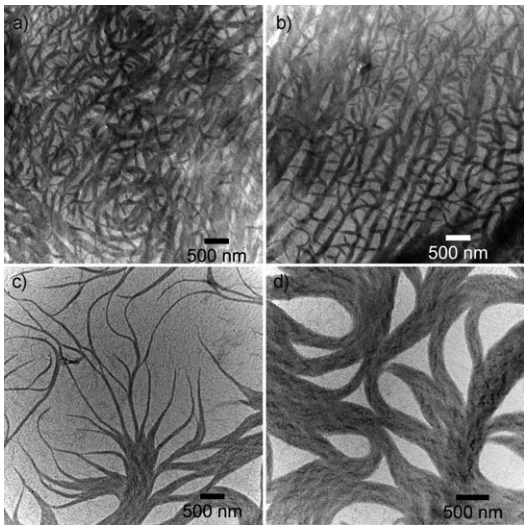

Figure 5. TEM images of macrocycle **1** with $NaBF_4$. a,b) The solvent was evaporated within 10 s at $T=92$ °C. c,d) The sample was dried inside a vial (in 80–90 min), which helped to slow down the evaporation of the solvent.

ogies observed in amphiphiles and block copolymers.[26] The evaporation rate can be used to control the length of the fibers prepared.

To summarize for Na^+, macrocycle **1** binds Na^+ in its interior to form a highly charged polymer, where alkali metals are bound to the macrocycles through Na–O interactions. These aggregates further condense into a much larger nanofibrillar bundle through electrostatic interactions between the anions and the polyelectrolyte. Potassium salts behave similarly, though the fiber quality is generally poorer than for sodium. This electrostatic self-assembly is reminiscent of the organization of actin filaments, which have supramolecular structures that are still poorly understood and not easily mimicked by synthetic models.[27]

With NH_4BF_4 used in place of $NaBF_4$, we see an additional level of hierarchy. Spectroscopically, NH_4^+ behaves very similarly to Na^+ when added to a solution of macrocycle **1**, forming 1D polymeric structures with the NH_4^+ cations bonded through hydrogen bonds in the interior of the macrocycles.[24] Remarkably, the nanofibers further assemble into bundles (microfibers) with diameters of microns and lengths of millimeters—they look like (orange) hair. Figure 6a shows an optical micrograph of the microfibrils; under crossed polarizers the samples are birefringent, indicating the fibers are anisotropic (see Figure S2 in the Supporting Information). It is noteworthy that each individual "hair" observed under the optical microscope is in fact a bundle of nanofibers. When deposited on a TEM grid, we can see nanofibers with diameters of approximately 200 nm (Figure 6b and c). This feature can be seen clearly by SEM (Figure 6d and e) and AFM (Figure 6f and g). Similar structures were observed with a shorter chain analogue of macrocycle **1** (with butyloxy substituents) when combined with NH_4BF_4.

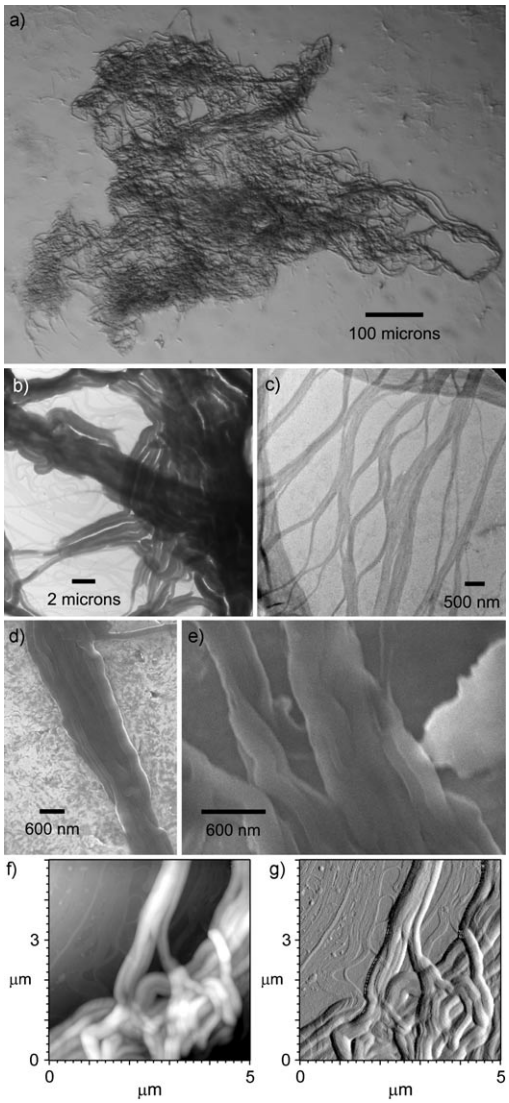

Figure 6. a) Optical, b,c) TEM, d,e) SEM, and f,g) AFM (height trace and amplitude trace, respectively) images of macrocycle **1** with NH_4BF_4. The sample has been negatively stained with chromium for better contrast in e).

In fact, these structures can be assembled directly from the precursors of macrocycle **1** (4,5-dihexyloxyphenylenediamine (**3**) and 3,6-diformylcatechol) with addition of NH_4BF_4, demonstrating another level of hierarchy in the one-pot assembly. The microfibers are similar to those obtained directly from macrocycle **1**, but shorter and finer. We attribute the size difference to the presence of oligomers that can act as impurities and interfere with fiber formation. Thus, we have observed a four-level hierarchical assembly that spans six orders of magnitude in length (from nm to mm) whereby the precursors of macrocycle **1** (dimensions of ca. 0.5 nm) react to form macrocycle **1** (diameter of ca. 2–3 nm), which assembles into an electrolytic polymer, then further organizes into nanofibers and microfibers (Figure 7). The graphic representation illustrates the self-assembly, but

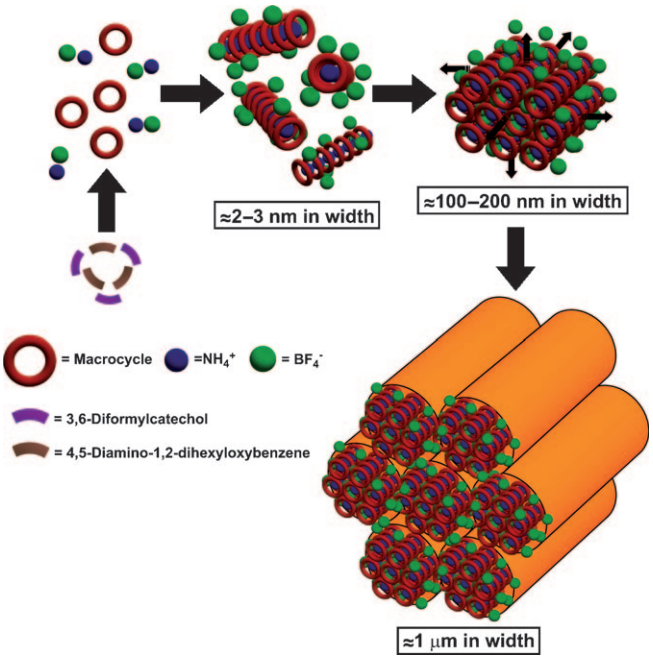

Figure 7. Graphical representation of the four-level hierarchical assembly. In the first step, dialdehyde and diamine precursors assemble into macrocycles. Upon reaction with NH_4BF_4, these macrocycles form polyelectrolytes that organize into nanofibers. In the final step, the nanofibers bundle into microfibers.

may be an oversimplification as both the longitudinal and transverse assembly could occur simultaneously.

Conclusion

Schiff base macrocycles having a central crown ether like interior were combined with alkali-metal and ammonium salts to generate fibrous structures. The nanofibers and microfibers formed by ion-induced hierarchical self-assembly of the macrocycles with $NaBF_4$ and NH_4BF_4 were extensively studied by solid-state NMR spectroscopy, TEM, SEM, and AFM, and with an optical microscope. It is believed that the cations first bind to the interior of the macrocycles to form one-dimensional aggregates that are surrounded by the counteranions of the salts on the outside. Through electrostatic interactions, these highly charged polymers then further organize into nanofibers or microfibers. It was also found that dimensions of the fibers are affected by the evaporation rate of the solvent. This hierarchical, structural organization is similar to the construction of guanosine-based fibrils and other fibrous structures from nature, and may offer a model for the hierarchical construction of biomimetic materials. Electrostatic self-assembly of nanofibers may prove useful for preparing functional materials and for understanding organization in biological materials.

Experimental Section

See the Supporting Information for additional experimental details and supporting spectra.

Preparation of 2,3-dimethoxytriptycene (5): A mixture of 2,3-dibromotriptycene (1.00 g, 2.44 mmol), copper(I) bromide (0.079 g, 0.55 mmol), sodium methoxide in methanol (25 wt%, 5 mL, 22 mmol), ethyl acetate (0.5 mL), and toluene (10 mL) was heated at reflux for 18 h. The solution was cooled to room temperature then quenched with the addition of water. After extracting the aqueous layer with dichloromethane, the combined organic layers were dried over anhydrous magnesium sulfate and filtered. The solvent was removed by rotary evaporation to give compound **5** (0.652 g, 85%) as a white solid. ^{1}H NMR (400 MHz, $CDCl_3$): $\delta = 7.37$ (m, 4H; aromatic CH), 7.03 (s, 2H; aromatic CH), 6.99 (m, 4H; aromatic CH), 5.35 (s, 2H; bridgehead H), 3.84 ppm (s, 6H; OCH_3). The ^{1}H NMR data are consistent with the literature values.[28]

Preparation of 1,4-diformyl-2,3-dimethoxytriptycene (6): Anhydrous *N*,*N*,*N*′,*N*′-tetramethyl-1,2-ethylenediamine (TMEDA) (5.30 mL, 35.3 mmol) was added to a solution of 2,3-dimethoxytriptycene (**5**) (4.589 g, 14.7 mmol) in anhydrous diethyl ether (20 mL). The cloudy solution was cooled to 0°C, butyllithium (1.6 M in hexanes, 40 mL, 58.8 mmol) was added dropwise over 30 min, and the brown suspension was then stirred for 16 h at ambient temperature. Anhydrous DMF (5.10 mL, 66.0 mmol) was added and the suspension was stirred for 30 min, followed by acidification with dilute hydrochloric acid and extraction with diethyl ether. The combined organic layers were dried with sodium sulfate, filtered, and the solvent was removed by rotary evaporation. The crude product was then purified by chromatography on silica gel (2:1 hexanes/methylene chloride) to elute the first yellow band. Rotary evaporation of the yellow solution yielded compound **6** (2.285 g, 42%) as a yellow solid. M.p. 190–192°C; ^{1}H NMR (400 MHz, $CDCl_3$): $\delta = 10.57$ (s, 2H; C(O)H), 7.46 (m, 4H; aromatic CH), 7.04 (m, 4H; aromatic CH), 6.86 (s, 2H; bridgehead *H*), 3.91 ppm (s, 6H; OCH_3); ^{13}C NMR (100.6 MHz, $CDCl_3$): $\delta = 191.9$ (C(O)H), 152.8, 144.6, 144.1, 129.1, 125.6, 124.3 (aromatic C), 62.2 (OCH_3), 47.9 ppm (bridgehead C); IR (neat): $\tilde{\nu} = 3004$, 2972, 2937, 2858, 1687, 1562, 1444, 1379, 1300, 1260, 1132, 1156, 1069, 1013, 986, 946, 746, 578 cm^{-1}; UV/Vis (CH_2Cl_2): λ_{max} (ε) = 273 (2.2×10^4), 278 (2.2×10^4), 373 nm (7.8×10^3 cm^{-1} M^{-1}); APCI-MS: *m*/*z*: 371 ($[M+H]^+$); elemental analysis calcd (%) for $C_{24}H_{18}O_4$ (**6**): C 77.82, H 4.90; found: C 77.61, H 4.85.

Preparation of 1,4-diformyl-2,3-dihydroxytriptycene (4): 1,4-Diformyl-2,3-dimethoxytriptycene (**6**) (2.285 g, 6.17 mmol) was dissolved in anhydrous methylene chloride (200 mL). The yellow solution was cooled to 0°C and boron tribromide (2.60 mL, 27.5 mmol) was added to give a fuming pink solution. After the reaction mixture was stirred at ambient temperature for 16 h, the solution was poured onto ice and extracted with methylene chloride. The combined organic fractions were dried with magnesium sulfate, filtered, and the solvent was removed by rotary evaporation to yield compound **4** (1.962 g, 93%) as an orange solid. M.p. decomposed around 220°C; ^{1}H NMR (400 MHz, $CDCl_3$): $\delta = 10.80$ (s, 2H; OH), 10.69 (s, 2H; C(O)H), 7.44 (m, 4H; aromatic CH), 7.07 (m, 4H; aromatic CH), 6.23 ppm (s, 2H; bridgehead H); ^{13}C NMR (100.6 MHz, $CDCl_3$): $\delta = 193.5$ (C(O)H), 147.0, 144.1, 139.7, 125.9, 123.8, 119.4 (aromatic *C*), 47.3 ppm (bridgehead *C*); IR (neat): $\tilde{\nu} = 3041$, 2996, 2922, 2852, 1644, 1556, 1458, 1436, 2895, 1273, 1198, 962, 921, 761, 675, 625, 600, 568 cm^{-1}; UV/Vis (CH_2Cl_2): λ_{max} (ε) = 253 (6.5×10^3), 294 (1.9×10^4), 453 nm (4.9×10^3 cm^{-1} M^{-1}); ESI-MS: *m*/*z*: 341.3 ($[M-H]^-$); elemental analysis calcd (%) for $C_{22}H_{14}O_4$ (**4**): C 77.18, H 4.12; found: C 76.83, H 4.19.

Preparation of triptycene-based Schiff base macrocycle 2: 1,4-Diformyl-2,3-dihydroxytriptycene (**4**) (0.035 g, 0.10 mmol) was added to a solution of 4,5-diamino-1,2-dihexyloxybenzene (**3**) (0.032 g, 0.10 mmol) in acetonitrile (6 mL). The deep red solution was stirred at 90°C for 14 h. After cooling to room temperature, it was kept at −10°C for 48 h to give a red precipitate. The solid was filtered and dried under vacuum to yield macrocycle **2** (0.032 g, 51%) as an orange solid. M.p. did not melt at 260°C; ^{1}H NMR (400 MHz, $CDCl_3$): $\delta = 13.04$ (s, 6H; OH), 9.27 (s, 6H; CH=N), 7.18 (m, 12H; aromatic CH), 7.00 (s, 6H; aromatic CH), 6.80 (m,

12H; aromatic CH), 5.83 (s, 6H; bridgehead H), 4.23 (t, 12H; OCH_2), 1.97 (m, 12H; CH_2), 1.62 (m, 12H; CH_2), 1.45 (m, 24H; CH_2), 0.98 ppm (t, 18H; CH_3); ^{13}C NMR (100.6 MHz, $CDCl_3$): $\delta = 159.3$ ($CH=N$), 149.4, 147.5, 145.0, 136.4, 136.0, 125.2, 123.2, 116.6, 107.0 (aromatic C), 70.4 (OCH_2), 48.5 (bridgehead C), 31.7, 29.4, 25.8, 22.7 (CH_2), 14.1 ppm (CH_3); IR (neat): $\tilde{\nu} = 3726$, 3708, 3627, 2925, 2854, 1606, 1506, 1462, 1426, 1375, 1304, 1257, 1173, 1115, 990, 759, 741, 624 cm^{-1}; UV/Vis (CH_2Cl_2): λ_{max} (ε) = 284 (5.8×10^4), 330 (7.1×10^4), 417 nm (1.2×10^5 $cm^{-1}M^{-1}$); ESI-MS: m/z: 1844.6 ($[M+H]^+$), 1867.6 ($[M+Na]^+$), 1883.4 ($[M+K]^+$); elemental analysis calcd (%) for $C_{120}H_{128}O_{13}N_6$ ($\mathbf{2}\cdot H_2O$): C 77.39, H 6.93, N 4.51; found: C 77.63, H 7.28, N 4.52.

Sample preparation of [Na·1]BF_4 for TEM imaging: Schiff base macrocycle **1** (1.5 mg, 1.1 μmol) was dissolved in chloroform (1 mL) and was mixed with an excess amount of sodium tetrafluoroborate (50 mg, 4.5 mmol) for 5 s to give a dark red solution. The solution was allowed to stand for 5 min, before removing the excess sodium tetrafluoroborate by filtration through a Kimwipe pad. The dark red solution was then diluted to half of its concentration before drop-casting onto the formvar carbon-coated grid. The coated grid was dried at ambient conditions. To prepare the sample with rapid evaporation, the coated grid was dried at 92 °C in 10 s. To prepare the sample with slow evaporation, the coated grid was dried in a partially closed vial at ambient temperature in 80–90 min.

Preparation of the microfibrils from macrocycle 1 and NH_4BF_4: Schiff base macrocycle **1** (1.0 mg; 0.76 μmol) was dissolved in chloroform (1.5 mL) and was mixed with an excess amount of ammonium tetrafluoroborate (20 mg, 1.9 mmol) for 5 s to give a dark red solution. The excess salt was then removed by filtration to give a brown solution. After 30 min, the solution became light brown and a brown precipitate was observed. Over time, the solution became lighter in color, and more precipitate could be obtained. This brown precipitate was found to be microfibrils when observed under an optical microscope and by AFM.

Acknowledgements

We thank the Natural Sciences and Engineering Research Council (NSERC) of Canada and UBC for funding. We thank Amanda Gallant who first prepared compound **6** in our laboratory. We also thank Timothy Kelly and Kevin Shopsowitz for obtaining the SEM images, and Tissaphern Mirfakhrai for obtaining the AFM images. We are grateful to Usama Al-Atar for performing the particle size measurements.

[1] a) P. Fratzl, R. Weinkamer, *Prog. Mater. Sci.* **2007**, *52*, 1263–1334; b) C. Sanchez, H. Arribart, M. M. Giraud Guille, *Nat. Mater.* **2005**, *4*, 277–288; c) E. Dujardin, S. Mann, *Adv. Mater.* **2002**, *14*, 775–788; d) I. A. Aksay, S. Weiner, *Curr. Opin. Solid State Mater. Sci.* **1998**, *3*, 219–220.

[2] P. Fratzl, *Curr. Opin. Colloid Interface Sci.* **2003**, *8*, 32–39.

[3] a) J. M. Gosline, M. E. DeMont, M. W. Denny, *Endeavour* **1986**, *10*, 37–43; b) F. Vollrath, D. P. Knight, *Nature* **2001**, *410*, 541–548.

[4] a) J. W. Orberg, L. Klein, A. Hiltner, *Connect. Tissue Res.* **1982**, *9*, 187–193; b) K. Okuyama, *Connect. Tissue Res.* **2008**, *49*, 299–310.

[5] N. A. Campbell, *Biology*, Benjamin/Cummings, Redwood City, **1993**, p. 785.

[6] a) J. D. Hartgerink, E. Beniash, S. I. Stupp, *Science* **2001**, *294*, 1684–1688; b) D. González-Rodríguez, J. L. J. van Dongen, M. Lutz, A. L. Spek, A. P. H. J. Schenning, E. W. Meijer, *Nat. Chem.* **2009**, *1*, 151–155; c) J. P. Hill, W. Jin, A. Kosaka, T. Fukushima, H. Ichihara, T. Shimomura, K. Ito, T. Hashizume, N. Ishii, T. Aida, *Science* **2004**, *304*, 1481–1483; d) S. Park, J.-H. Lim, S.-W. Chung, C. A. Mirkin, *Science* **2004**, *303*, 348–351; e) J. J. L. M. Cornelissen, J. J. J. M. Donners, R. de Gelder, W. S. Graswinckel, G. A. Metselaar, A. E. Rowan, N. A. J. M. Sommerdijk, R. J. M. Nolte, *Science* **2001**, *293*, 676–680; f) F. A. Aldaye, P. K. Lo, P. Karam, C. K. McLaughlin, G. Cosa, H. F. Sleiman, *Nat. Nanotechnol.* **2009**, *4*, 349–352.

[7] a) J. J. L. M. Cornelissen, M. Fischer, N. A. J. M. Sommerdijk, R. J. M. Nolte, *Science* **1998**, *280*, 1427–1430; b) S. A. Jenekhe, X. L. Chen, *Science* **1999**, *283*, 372–375; c) V. Percec, B. C. Won, M. Peterca, P. A. Heiney, *J. Am. Chem. Soc.* **2007**, *129*, 11265–11278; d) V. Percec, M. R. Imam, M. Peterca, D. A. Wilson, P. A. Heiney, *J. Am. Chem. Soc.* **2009**, *131*, 1294–1304; e) W.-D. Jang, T. Aida, *Macromolecules* **2004**, *37*, 7325–7330.

[8] D. T. Bong, T. D. Clark, J. R. Granja, M. R. Ghadiri, *Angew. Chem.* **2001**, *113*, 1016–1041; *Angew. Chem. Int. Ed.* **2001**, *40*, 988–1011.

[9] a) M. Fischer, G. Lieser, A. Rapp, I. Schnell, W. Mamdouh, S. De Feyter, F. C. De Schryver, S. Höger, *J. Am. Chem. Soc.* **2004**, *126*, 214–222; b) S. Höger, *Chem. Eur. J.* **2004**, *10*, 1320–1329; c) J. Zhang, J. S. Moore, *J. Am. Chem. Soc.* **1994**, *116*, 2655–2656.

[10] a) S. L. Forman, J. C. Fettinger, S. Pieraccini, G. Gottarelli, J. T. Davis, *J. Am. Chem. Soc.* **2000**, *122*, 4060–4067; b) A. J. Helsel, A. L. Brown, K. Yamato, W. Feng, L. Yuan, A. J. Clements, S. V. Harding, G. Szabo, Z. Shao, B. Gong, *J. Am. Chem. Soc.* **2008**, *130*, 15784–15785.

[11] a) S.-i. Kawano, S.-i. Tamaru, N. Fujita, S. Shinkai, *Chem. Eur. J.* **2004**, *10*, 343–351; b) K. Balakrishnan, A. Datar, W. Zhang, X. Yang, T. Naddo, J. Huang, J. Zuo, M. Yen, J. S. Moore, L. Zang, *J. Am. Chem. Soc.* **2006**, *128*, 6576–6577; c) K. Nakao, M. Nishimura, T. Tamachi, Y. Kuwatani, H. Miyasaka, T. Nishinaga, M. Iyoda, *J. Am. Chem. Soc.* **2006**, *128*, 16740–16747.

[12] a) L. Brunsveld, B. J. B. Folmer, E. W. Meijer, R. P. Sijbesma, *Chem. Rev.* **2001**, *101*, 4071–4098; b) T. Akutagawa, T. Ohta, T. Hasegawa, T. Nakamura, C. A. Christensen, J. Becher, *Proc. Natl. Acad. Sci. USA* **2002**, *99*, 5028–5033; c) A. Petitjean, L. A. Cuccia, M. Schmutz, J.-M. Lehn, *J. Org. Chem.* **2008**, *73*, 2481–2495; d) S. Margadonna, K. Prassides, Y. Iwasa, Y. Taguchi, M. F. Craciun, S. Rogge, A. F. Morpurgo, *Inorg. Chem.* **2006**, *45*, 10472–10478; e) A. Petitjean, L. A. Cuccia, J.-M. Lehn, H. Nierengarten, M. Schmutz, *Angew. Chem.* **2002**, *114*, 1243–1246; *Angew. Chem. Int. Ed.* **2002**, *41*, 1195–1198.

[13] S. Höger, K. Bonrad, A. Mourran, U. Beginn, M. Möller, *J. Am. Chem. Soc.* **2001**, *123*, 5651–5659.

[14] V. Sidorov, F. W. Kotch, M. El-Kouedi, J. T. Davis, *Chem. Commun.* **2000**, 2369–2370.

[15] a) X. Zhang, Y. Wang, X. Chen, W. Yang, *Mater. Lett.* **2008**, *62*, 1613–1616; b) J. F. Quinn, A. P. R. Johnston, G. K. Such, A. N. Zelikin, F. Caruso, *Chem. Soc. Rev.* **2007**, *36*, 707–718; c) G. Decher, *Science* **1997**, *277*, 1232–1237; d) S.-H. Lee, S. Balasubramanian, D. Y. Kim, N. K. Viswanathan, S. Bian, J. Kumar, S. K. Tripathy, *Macromolecules* **2000**, *33*, 6534–6540; e) S. Balasubramanian, X. Wang, H. C. Wang, K. Yang, J. Kumar, S. K. Tripathy, L. Li, *Chem. Mater.* **1998**, *10*, 1554–1560.

[16] a) Y. Guan, S.-H. Yu, M. Antonietti, C. Böttcher, C. F. J. Faul, *Chem. Eur. J.* **2005**, *11*, 1305–1311; b) K. Adachi, H. Irie, T. Sato, A. Uchibori, M. Shiozawa, Y. Tezuka, *Macromolecules* **2005**, *38*, 10210–10219; c) M. Annaka, K. Morishita, S. Okabe, *J. Phys. Chem. B* **2007**, *111*, 11700–11707; d) J.-F. Berret, B. Vigolo, R. Eng, P. Hervé, I. Grillo, L. Yang, *Macromolecules* **2004**, *37*, 4922–4930.

[17] Z. Wang, K. J. Ho, C. J. Medforth, J. A. Shelnutt, *Adv. Mater.* **2006**, *18*, 2557–2560.

[18] a) N. Kimizuka, *Adv. Polym. Sci.* **2008**, *219*, 1–26; b) O. Ikkala, R. H. A. Ras, N. Houbenov, J. Ruokolainen, M. Pääkkö, J. Laine, M. Leskelä, L. A. Berglund, T. Lindström, G. ten Brinke, H. Iatrou, N. Hadjichristidis, C. F. J. Faul, *Faraday Disc.* **2009**, *143*, 95–107.

[19] a) J. T. Davis, *Angew. Chem.* **2004**, *116*, 684–716; *Angew. Chem. Int. Ed.* **2004**, *43*, 668–698; b) J. T. Davis, G. P. Spada, *Chem. Soc. Rev.* **2007**, *36*, 296–313.

[20] L. E. Buerkle, Z. Li, A. M. Jamieson, S. J. Rowan, *Langmuir* **2009**, *25*, 8833–8840, and references therein.

[21] A. Wong, R. Ida, L. Spindler, G. Wu, *J. Am. Chem. Soc.* **2005**, *127*, 6990–6998.

[22] M. P. H. Lee, G. N. Parkinson, P. Hazel, S. Neidle, *J. Am. Chem. Soc.* **2007**, *129*, 10106–10107.

[23] A. J. Gallant, J. K.-H. Hui, F. E. Zahariev, Y. A. Wang, M. J. MacLachlan, *J. Org. Chem.* **2005**, *70*, 7936–7946.

[24] A. J. Gallant, M. J. MacLachlan, *Angew. Chem.* **2003**, *115*, 5465–5468; *Angew. Chem. Int. Ed.* **2003**, *42*, 5307–5310.

[25] a) R. van Hameren, A. M. van Buul, M. A. Castriciano, V. Villari, N. Micali, P. Schön, S. Speller, L. Monsù Scolaro, A. E. Rowan, J. A. A. W. Elemans, R. J. M. Nolte, *Nano Lett.* **2008**, *8*, 253–259; b) R. van Hameren, P. Schön, A. M. van Buul, J. Hoogboom, S. V. Lazarenko, J. W. Gerritsen, H. Engelkamp, P. C. M. Christianen, H. A. Heus, J. C. Maan, T. Rasing, S. Speller, A. E. Rowan, J. A. A. W. Elemans, R. J. M. Nolte, *Science* **2006**, *314*, 1433–1436.

[26] a) L. Hsu, G. L. Cvetanovich, S. I. Stupp, *J. Am. Chem. Soc.* **2008**, *130*, 3892–3899; b) M. O. Guler, S. Soukasene, J. F. Hulvat, S. I. Stupp, *Nano Lett.* **2005**, *5*, 249–252; c) L. Shen, H. Wang, G. Guerin, C. Wu, I. Manners, M. A. Winnik, *Macromolecules* **2008**, *41*, 4380–4389; d) G. Liu, *Adv. Mater.* **1997**, *9*, 437–439.

[27] a) J. Hu, A. Matzavinos, H. G. Othmer, *J. Stat. Phys.* **2007**, *128*, 111–138; b) P. Kraikivski, B. M. Slepchenko, I. L. Novak, *Phys. Rev. Lett.* **2008**, *101*, 128102–1–128102–4; c) M.-F. Carlier, S. Wiesner, D. Pantaloni, *J. Biol. Phys.* **2002**, *28*, 327–333; d) H. J. Kwon, A. Kakugo, K. Shikinaka, Y. Osada, J. P. Gong, *Biomacromolecules* **2005**, *6*, 3005–3009.

[28] K. Gong, X. Zhu, R. Zhao, S. Xiong, L. Mao, C. Chen, *Anal. Chem.* **2005**, *77*, 8158–8165.

Received: October 2, 2009
Published online: January 11, 2010

